Modeling of pancake frying with non-uniform heating source applied to domestic cookers

F. Sanz-Serrano[a,*], C. Sagues[a], A.H. Feyissa[b], J. Adler-Nissen[b], S. Llorente[c]

[a]*I3A Universidad de Zaragoza, Mariano Esquillor s/n, Zaragoza 50018, Spain*
[b]*Food Production Engineering, National Food Institute, Søltofts Plads, Building 227, 2800 Kgs. Lyngby, DTU, Denmark*
[c]*Research and Development Department, Induction Technology, Product Division Cookers, BSH Home Appliances Group, Avenida de la Industria 49, Zaragoza 50016, Spain*

Abstract

The design of domestic cooking stoves is usually optimized by performing time-consuming cooking experiments, often using frying of pancakes as a standard. Simulation of cooking processes may reduce the number of experiments used in the development of the cooking stoves, saving time and resources. In this work we propose a model of contact frying of pancakes in domestic cookers, particularly in induction hobs and radiant cookers, in which the heating of the cooking vessels can be non-uniform. This non-uniformity is unavoidable in practice, but it can be reduced by optimizing the design of the cooker. The proposed model combines heat and mass transfer phenomena, and also includes the correlation between the browning development and the temperature distribution, the local water content and the cooking time. The model has been also validated through experiments using a commercial induction hob and a radiation stove. With this model the color of the cooked pancakes can be predicted, taking into account also uneven heating, and through simulations the design of the cooker can be improved.

Keywords: Modeling; pancake frying; non-uniform heating; browning development; domestic cooking.

1. Introduction

* Corresponding author. Tel.:+34-669-917-886.
E-mail addresses: fer.sanz@unizar.es (F. Sanz-Serrano), csagues@unizar.es (C. Sagues), abhfe@food.dtu.dk (A.H. Feyissa), jadn@food.dtu.dk (J. Adler-Nissen), sergio.llorente@bshg.com (S. Llorente).

It is widely known that a non-uniform heating of the base of an even well-designed frying pan results in a non-uniform cooking of the food, where overcooked zones as well as raw zones may appear. This undesirable effect is critical and must be taken into account when designing cooking stoves, because the type and configuration of the heating source determines the resultant temperature distribution in the pan.

In the case of induction cooktops, due to the geometry of the coil, a non-uniform current density distribution is induced in the pan material (Carretero et al., 2015; Pham et al., 2012), which may cause significant temperature gradients. This temperature unevenness is aggravated under certain common cooking conditions in the users' kitchens. For example, when the cooking vessel is bigger than the coil, the outer area of the base remains colder than the center.

As a part of the quality control of the induction hobs, manufacturers perform different tests with each hob variant under real cooking conditions, such as contact frying of pancakes or steaks, deep frying of chips or croquettes and water boiling (AEN/CT N 213 Electrodomesticos, 2014). These standardized tests are developed to evaluate different features of the cooker performance, such as efficiency, energy consumption, durability or cooking uniformity. The most common test used for the evaluation of the heating uniformity is pancake frying, in which the temperature distribution is indirectly analyzed by studying the differences in the browning of the pancake face in contact with the pan during the frying process. Such tests imply spending high amounts of time and resources, which could be in fact reduced by using other direct methods for measuring the temperature distribution, such as an infrared (IR) camera and heating an empty pan. However, the evaluation considering the food is necessary for controlling the quality of the stoves, since the normal functioning in the final user's home is reproduced, and the suitability of the cooker performance can easily be confirmed. For this reason the development of theoretical models of different cooking situations is of great interest, since the result of the cooking experiments can be predicted in an earlier stage of the design process, saving costs of prototypes and experiments. Since one of the most critical tests for evaluating the cooking uniformity is the contact frying of thin pancakes, this type of food will be studied in the present work.

Some contact frying models have been presented in previous works, where focus has been to study the food properties such as heat conductivity, or to estimate the effects of the cooking process such as mass loss, local temperature evolution or shrinkage effects. For example Zorrilla and Singh (2003) proposed a two-dimensional

model of contact frying of meat patties, Gupta (2001) studied the contact baking of flat Indian bread in a continuous oven with a simplified model, Feyissa et al. (2011) proposed a theoretical model of contact frying of thick pancakes, considering coupled heat and mass transfer phenomena. In all these works, the temperature distribution of the hot surface (double grill, steel slats, baking plate) was uniform, which is the best-case situation in a contact cooking process. However when considering a domestic cooker, the heat source typically provides a non-uniform heat distribution, which may lead to an uneven temperature distribution in the cooking vessel. Hence, it becomes necessary to include a non-uniform heat source in the new model.

As mentioned before, the evaluation of the heating uniformity of domestic cookers is carried out through the experimental measurement of browning differences in cooked pancakes, which is not only a way of taking into account the user's perception of quality, but also an indirect way of analyzing the temperature distribution in the cooker, since browning is the consequence of the temperature evolution, time and product composition. The browning of bakery products is the result of a combination of Maillard reactions and caramelization (Martins et al., 2000; Purlis, 2010). The color formation in different types of food products using different cooking techniques (meat, bread or biscuit) has been modeled with a basis in chemical kinetics theory and empirical correlations, giving a good agreement between the measured color and the predicted color after a determined cooking process (Broyart et al., 1998; Purlis and Salvadori, 2009). A similar approach can be used for modeling the color formation in a contact frying process using a domestic stove, taking into account a non-uniform temperature distribution. Knowing the evolution of the temperature and water content, the resulting color distribution at a given time may then be predicted and used for the evaluation of the heating performance of the cooker.

The objective of the present work is to establish a pancake frying model which includes a non-uniform power distribution transferred by a domestic cooker to the base of the cooking vessel. It allows the calculation of the temperature and water content in the food as well as the resulting color distribution. This non-uniform heating condition has barely been considered in previous works related to industrial applications of food engineering, where the heating source and/or the cooking surface are usually designed in order to minimize the temperature gradients. However in domestic cookers, due to the wide variability of types of pans existing in the market, a perfectly uniform temperature distribution is often impossible to obtain. Therefore, the contributions of this work are the proposed transport model with a non-uniform heat source and an experimentally determined color correlation between the

75 browning of the pancake surface and the frying process (temperature, water content and time). The proposed model
76 makes possible to simulate the frying process and obtain the color distribution, helping to predict if the configuration
77 of a certain cooker is optimal. This would improve the design process of cooktops and save development costs. In
78 order to adjust the proposed model, experiments of controlled cooking using a uniform-heating rig (Ashokkumar
79 and Adler-Nissen, 2011) have been carried out, and the obtained results have been extrapolated to the real case of
80 domestic cookers. The model has been also validated through experiments using a commercial induction hob and a
81 radiation stove.

82 **2. Theory**

83 The contact frying of pancakes can be modeled as a coupled heat and mass transfer problem (Feyissa et al.,
84 2011). The heat transferred from the base of the frying-pan to the pancake dough increases its temperature, and the
85 water present in the dough starts to evaporate, absorbing a high amount of energy during the phase change. The
86 gradient of the concentration of liquid water and vapor produces a mass transfer effect due to diffusion inside the
87 product, which also affects the thermal properties and, therefore, the temperature evolution.

88 *2.1. Two-dimensional model of pancake cooking*

89 The proposed model is based on the previous work from Feyissa et al. (2011), in which a one-dimensional model
90 of the heat and mass transfer problem for a thick pancake (8 mm) was presented. In the present work a two-
91 dimensional axisymmetric model is used, in order to include the non-uniform heating of the cooking vessel.
92 Moreover, the pancake thickness is closer to the traditional French pancake (3 mm thick) used in the standardized
93 tests. Like in Feyissa et al. (2011) it is assumed that the temperature-induced chemical reactions of the solid
94 components, such as the egg protein coagulation or the color formation, have no influence on the bulk material
95 properties. The model is implemented in COMSOL Multiphysics® 5.0, which is based on the Finite Element
96 Method (FEM) for the numerical simulations. This implementation allows the selection of the input conditions such
97 as the power source, and the material properties. Therefore similar models can be used to simulate the frying process
98 using different heating technologies. In this work an induction hob which directly heats the cooking vessel placed on
99 a ceramic glass plate has been considered (Fig. 1 (a)), but also a heating rig with a hot surface at uniform
100 temperature, used in the previous works by Ashokkumar and Adler-Nissen (2011) and by Feyissa et al. (2011), Fig.

1 (b). The uniform-heating rig model will be used to identify the model parameters and develop the color formation correlations, and the results obtained can then be used in a more complex model with a non-uniform heating.

2.1.1. Heat transfer model

The thermal system which has been considered consists of a pancake product inside a frying disk with an outer rim. The disk is placed on a ceramic glass plate in the case of the induction hob and on an aluminum slab in the case of the uniform-heating rig (cf. also section 3.1.). The temperature evolution of the frying disk heated by induction is given by the governing equation:

$$P + \lambda \nabla^2 T = \rho C \frac{\partial T}{\partial t} \tag{1}$$

where P is the volumetric power density generated by the inductor in $\mathrm{W/m^3}$. The second term is the effect of heat conduction, where $\nabla^2 T$ is the Laplacian of the temperature T in K and λ is the heat conductivity of the material with units $\mathrm{W/(m \cdot K)}$. The term on the right side is the variation of the energy stored in the system with time, where the material has density ρ with units $\mathrm{kg/m^3}$ and specific heat capacity C with units $\mathrm{J/(kg \cdot K)}$. The power term P disappears in the case of the uniform-heating rig, since the heat is transferred to the disk through the contact with the aluminum block, obtaining the governing equation:

$$\lambda \nabla^2 T = \rho C \frac{\partial T}{\partial t} . \tag{2}$$

The heat transfer within the pancake domain is given by equation (3):

$$\lambda_p \nabla^2 T = \rho_p C_p \frac{\partial T}{\partial t} + Q_{evp} \tag{3}$$

where Q_{evp} in $\mathrm{W/m^3}$ is the heat sink corresponding to the water evaporation, λ_p, ρ_p and C_p are the product properties – the thermal conductivity, the density and the effective specific heat capacity, respectively.

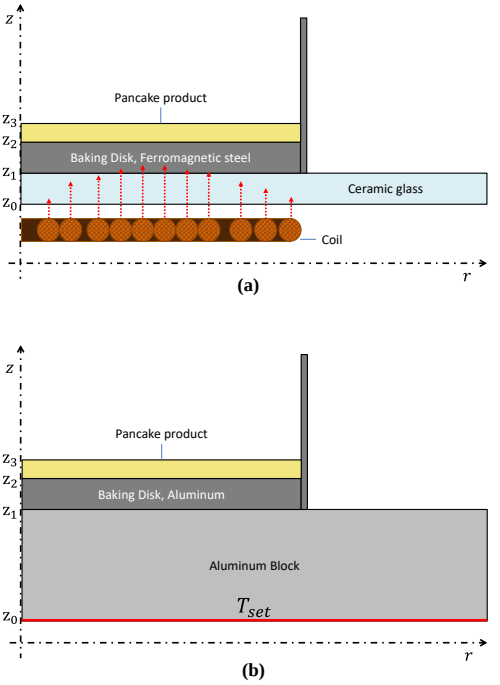

Fig. 1. Axisymmetric schemes of the pancake cooking model using different heating technologies: (a) induction heating with a non-uniform power distribution generated in the frying disk – symbolized with red arrows, (b) uniform-heating rig with aluminum block at controlled temperature T_{set} on the highlighted surface.

The energy absorbed by the water during the evaporation process is calculated as:

$$Q_{evp} = R_{evp} \cdot L_{evp} \tag{4}$$

where R_{evp} in $\mathrm{kg/(m^3 \cdot s)}$ is the mass evaporation rate, which is a function of temperature and water content, and $L_{evp} = 2.26 \cdot 10^6\ \mathrm{J/kg}$ is the water evaporation enthalpy at 100ºC and 1 atm. The evaporation rate R_{evp} is described by:

$$R_{evp} = \sigma_{evp} \cdot \rho_p \cdot \theta(T) \cdot \eta(x_l) \tag{5}$$

where σ_{evp} is the rate constant with units 1/s and $\theta(T), \eta(x_l)$ are functions used to model the complex phenomena which occur during the evaporation of the water in the pancake product. A similar expression to calculate R_{evp}, based on the Arrhenius equation, was presented by Feyissa et al. (2011). However, two slight modifications have been carried out in the present work. Firstly, the phase change coefficient introduced by Feyissa et al. (2011) has been reformulated for convenience, obtaining the equivalent exponential function $\theta(\mathrm{T})$, parameterized by the

evaporation temperature $T_{ev} = 373.15$ K and the dimensionless constant k_θ, as given by (6)

$$\theta(T) = \begin{cases} exp\left(k_\theta\left(1 - \frac{T_{ev}}{T}\right)\right) & 0 < T \leq T_{ev} \\ 1 & T_{ev} < T \end{cases}. \quad (6)$$

Secondly, instead of considering that the mass evaporation rate is proportional to the water content x_l, as stated in the work of Feyissa et al. (2011), the piecewise function $\eta(x_l)$ is defined as:

$$\eta(x_l) = \begin{cases} 0 & 0 \leq x_l \leq x_{l_{bnd}} \\ 1 & x_{l_{bnd}} < x_l \leq 1 \end{cases}. \quad (7)$$

The threshold water content, $x_{l_{bnd}} = 0.4$, takes into account the effect of the bound water present in the dough (Bushuk and Mehrotra, 1977; Ulbrich and Flöter, 2014) which cannot be evaporated during the cooking process. Thus, the evaporation rate remains constant with the water content provided that free water is present, and the evaporation stops when the threshold $x_{l_{bnd}}$ is reached, which is a more realistic approximation. In order to reduce computational problems associated with sharp changes of the values of $\theta(T)$ and $\eta(x_l)$, smoothed piecewise functions are used in the implementation in the FEM software.

In the case of the induction hob, the bottom surface of the glass ($z = z_0$) is considered adiabatic, because the temperature of the coil and the air beneath the glass is close to the temperature of the glass, and the heat losses are therefore negligible. In the case of the uniform-heating rig, the surface is documented to have a constant temperature T_{set} (Ashokkumar and Adler-Nissen, 2011).

The heat flux established through the bottom surface of the baking disk due to the contact with the ceramic glass in the induction hob is defined with a contact conductance h_c (Sanz-Serrano et al., 2016)

$$-\lambda_d \left.\frac{\partial T}{\partial z}\right|_{z=z_1} = -\lambda_g \left.\frac{\partial T}{\partial z}\right|_{z=z_1} = h_c \left(T_g - T_d\right)\big|_{z=z_1} \quad (8)$$

where T_d, T_g and λ_d, λ_g are the temperatures and heat conductivities of disk and glass, respectively. Equivalently, the contact conduction between the frying disk and the hot aluminum slab of the rig is

$$-\lambda_d \left.\frac{\partial T}{\partial z}\right|_{z=z_1} = -\lambda_s \left.\frac{\partial T}{\partial z}\right|_{z=z_1} = h_c \left(T_s - T_d\right)|_{z=z_1} \quad (9)$$

where T_s and λ_s are the temperature and heat conductivity of the hot slab.

On the disk top surface ($z = z_2$), in contact with the pancake, the heat flux continuity is considered, which is given by equation (10)

$$-\lambda_d \frac{\partial T}{\partial z}\Big|_{z=z_2} = -\lambda_p \frac{\partial T}{\partial z}\Big|_{z=z_2} . \quad (10)$$

On the top surface of the pancake and the glass (or the aluminum slab), and on the wall of the frying disk, heat losses due to natural convection and radiation are considered. The corresponding heat transfer coefficients are calculated from conventional empirical correlations by the FEM software, considering the geometry and ambient temperature (Bergman et al., 2011). For the pancake surface the convection coefficient is 8 W/m^{2}K, on the walls of the frying disk and on the glass (or the aluminum slab) the convection coefficient is 10 W/m^{2}K. The emissivity of the different materials is: 0.96 for the pancake (similar to water), 0.1 on the steel walls, 1 on the glass and 0.3 on the aluminum slab.

2.1.2. Mass transfer model

The mass transfer phenomenon only takes place inside the pancake domain and through the top surface of the pancake, in which the liquid water and vapor move mainly due to diffusion. The governing equations are similar to those appearing in Feyissa et al. (2011)

$$\rho_p \frac{\partial x_l}{\partial t} = \nabla \cdot \left(\rho_p \, D_l \nabla x_l\right) - R_{evp} \quad (11a)$$

$$\rho_p \frac{\partial x_v}{\partial t} = \nabla \cdot \left(\rho_p \, D_v \nabla x_v\right) + R_{evp} \quad (11b)$$

where $x_l + x_v + x_s = 1$ is a constraint. The mass fractions of the solid, liquid and vapor are x_s , x_l , x_v , expressed in kg of water/kg of sample, respectively. The diffusion coefficients are D_l , D_v with units m^2 s^{-1}, R_{evp} is the rate of water evaporation (which is water disappearance or the vapor generation rate), as defined in (5).

A null mass flux is considered through the boundaries in contact with the frying disk, and through the top surface of the pancake a mass flow of vapor is stated as the boundary condition

$$-D_v \frac{\partial x_v}{\partial z}\Big|_{z=z_3} = k_v \cdot \rho_p \cdot \left(x_v - x_{v_a}\right)\Big|_{z=z_3} \quad (12)$$

where k_v is a mass flux constant with units m/s and x_{v_a} is the humidity of the surrounding air, expressed in basis of

product mass, being x'_{v_a} the measured humidity in kg of vapor per kg of air and ρ_a the air density at ambient temperature

$$x_{v_a} = x'_{v_a} \frac{\rho_a}{\rho_p}. \tag{13}$$

2.1.3. Calculation of thermal properties

The thermal properties of the metal and the glass do not change significantly during the frying process. However, there is a strong dependence of the product properties with the water and vapor content, which change continuously due to the evaporation and mass transport phenomena. Thus, the local values of the pancake properties are calculated as a function of temperature and composition, which is stated by the mass fractions of the solid, liquid and vapor: x_s , x_l , x_v , solution of the mass transfer problem. The solid fraction is the aggregate of solid components in the dough (protein, fat, carbohydrate), obtained from the pancake recipe and from the food database of Saxholt et al. (2008).

To calculate the product density ρ_p, additive volumes are considered in the following expression extracted from (Nesvadba, 2014)

$$\rho_p = \left(\frac{x_l}{\rho_l} + \frac{x_s}{\rho_s} + \frac{x_v}{\rho_v}\right)^{-1} \tag{14}$$

ρ_l and ρ_s are the densities of the liquid water and the solid. The porosity (volume fraction of vapor) ε_v is obtained with

$$\varepsilon_v = \frac{x_v}{\rho_v}\rho_p = x_v \frac{R_g \cdot T}{pA \cdot M_w}\rho_p \tag{15}$$

where the ideal gas law is used in the calculation of the vapor density ρ_v, considering atmospheric pressure pA = 1atm (Datta, 2007a), the gas constant $R_g = 8.2 \cdot 10^{-2}$ atm L mol^{-1} K^{-1} and the molecular weight of vapor M_w = 18 g mol^{-1}. The local expansion of the pancake due to the additional volume filled with vapor can be calculated with

$$\alpha = \frac{x_{s_0} \cdot \rho_{p_0}}{x_s \cdot \rho_p} \tag{16}$$

where x_{s_0} , ρ_{p_0} are the initial solid mass fraction and the initial density.

186 The heat capacity C_p and the heat conductivity λ_p of the pancake are calculated with well-known expressions
187 according to Nesvadba (2014)

$$C_p = \sum_i x_i C_i$$
$$\frac{1}{\lambda_{p_\perp}} = \sum_i \frac{\varepsilon_i}{\lambda_i}$$
$$\lambda_{p_\parallel} = \sum_i \varepsilon_i \cdot \lambda_i$$
$$\lambda_p = g_\lambda \cdot \lambda_{p_\perp} + (1 - g_\lambda) \cdot \lambda_{p_\parallel} \quad (17)$$

188 where ε_i is the volume fraction and λ_i is the heat conductivity of each component. The value of the factor g_λ
189 depends on the porosity with the expression

$$g_\lambda = 0.04 + g_\varepsilon \cdot \varepsilon_v \quad (18)$$

190 which is similar to the one appearing in Nesvadba (2014) for porous food products. The sensitivity of the results is
191 significant with respect to the coefficient g_ε and its value must be determined experimentally.

192 *2.2. Browning development model*

193 The browning is the result of a combination of Maillard reactions and caramelization (Martins et al., 2000; Purlis,
194 2010). The evaluation of the progress of the browning process can be conveniently carried out with computer vision
195 systems, in which the variation of the color of the product surface is obtained from image processing tools. This
196 technique has recently become more common due to the advantages which offers with respect to other chemical
197 methods (Zheng et al., 2006). In particular, the lightness parameter L* of the standard color space CIE L*a* b* is
198 normally used (Gökmen et al., 2008; León et al., 2006; Zheng et al., 2006).

199 The Maillard reactions and the caramelization occur simultaneously and they can be integrated in a combined
200 model, which relates the color with the time, temperature and water content of the product (Purlis, 2010). In this
201 work, the browning model is based on first-order kinetics with the browning rate constant depending on temperature
202 and water content. The variation of the color component L* with time, as presented by Purlis (2010), is given by

$$\frac{dL^*}{dt} = -k\, L^* \quad (19)$$

where k is the browning rate constant, which depends on the temperature as stated in the Arrhenius' law

$$k = k_0\, exp\left(-\frac{A}{T}\right) \tag{20}$$

being k_o and A variables dependent on the water content in kg of water / kg of sample

$$k_0 = k_1 + \frac{k_2}{x_l}$$
$$A = A_1 + \frac{A_2}{x_l} \tag{21}$$

As it is known, the temperature and the water content also vary with time during the cooking process. However they can be calculated by means of the aforementioned numerical method based in FEM. For this reason, the solution of (19) can be obtained with the expression

$$L^* = L_o\, exp\left(\int_{t_0}^{t} -k_0\, exp\left(-\frac{A}{T}\right) dt\right) \tag{22}$$

which can be numerically obtained knowing the evolution of T and x_l with the time. The parameters, L_0, k_1, k_2, A_1, A_2 will be identified using experimental measurements of the color of pancakes cooked with the uniform-heating rig, using different cooking times and temperatures. For the remaining color components in the L*a*b* space, the suitability of similar equations with different parameter values will be discussed in section 3.3.

3. Experiments

The values of the parameters $\sigma_{ev}, k_\theta, g_\varepsilon, k_v, h_c, D_l, D_v$ which appear in the previously presented model of heat and mass transfer and the aforementioned parameters of the browning development model are unknown and therefore must be determined experimentally. In order to simplify the problem and increase the accuracy of the identification process, the experiments are performed using the aforementioned uniform-heating rig which provides a surface at a controlled, uniform temperature (Ashokkumar and Adler-Nissen, 2011). Under this condition the problem is simpler, as the effect of the uneven temperature distribution in the pan is avoided, and the color formation in the bottom surface of the pancake can be related to the controlled temperature.

3.1. Experimental set-up

The uniform-heating rig (Fig. 2) consists of a slab of aluminum of 30x30x2.5 cm^3 with isolated side faces and

heated from beneath by contact with an electric hotplate. Inside the slab there is a temperature probe, which feeds back data to a controller which allows the setting of the desired temperature (Ashokkumar and Adler-Nissen, 2011). The equipment rests on an electronic balance, with a precision of 0.1 g, and this allows the continuous recording of the mass loss. The frying disk employed in these experiments is an aluminum disk of 9 cm of diameter and 0.5 cm of thickness, with a non-stick PTFE coating, and the wall is a ring of stainless steel of the same internal diameter, 2.5 cm of height and 0.15 cm of thickness (Feyissa et al., 2015, 2011).

Fig. 2. Uniform-heating rig and balance.

In order to measure the pancake temperature, type T thermocouples of 0.75 mm of diameter are used with a PICO TC08 register. Two thermocouples are fixed through a cylindrical piece of PTFE with drills at the bottom and at 3.5 mm from the bottom. With this disposition the evolution of the temperature of the disk and of the top surface of the pancake can be measured. The bottom thermocouple is fixed to the disk surface 12 mm from the center, using thermo-resistant tape (KAPTON) and thermal conductive silicone, in order to improve the thermal contact between the sensor and the surface, Fig. 3. The PTFE piece fixates the thermocouples in the desired position. Due to its low conductivity ($0.25\ \mathrm{W/(m \cdot K)}$), similar to the pancake dough, it has little disturbing effect on the cooking process.

The pancake dough is prepared with the ingredients which appear in the standard (AEN/CT N 213 Electrodomesticos, 2014), which includes milk (53.3%), chicken egg (20.7%), wheat flour (25.8%) and salt (0.2%). The initial density is measured by weighing a known volume of dough, obtaining $\rho_{p_0} = 1110\ \mathrm{kg/m^3}$. The initial water content, estimated from the product composition and the water content of the constituents, appearing in Saxholt et al., (2008) is $x_{l_0} = 0.65\ \mathrm{kg\,water/kg\,sample}$, and the solid mass fraction is $x_{s_0} =$

242 0.35 kg solid/kg sample.

243 The desired temperature is set in the control unit of the uniform-heating rig and it is allowed to equilibrate for 20
244 minutes. The standard states that the temperature of the frying disk should be 235ºC±5ºC for a right cooking result.
245 However in order to obtain a wider range of data different temperatures are tested, between 180ºC and 260ºC. This
246 range is defined considering the temperature differences which can appear when heating a frying pan with an
247 induction hob in a normal cooking process. The higher limit is stated due to the maximum temperature which the
248 PTFE coating resists without starting to degrade (Fluoroproducts, 1996).

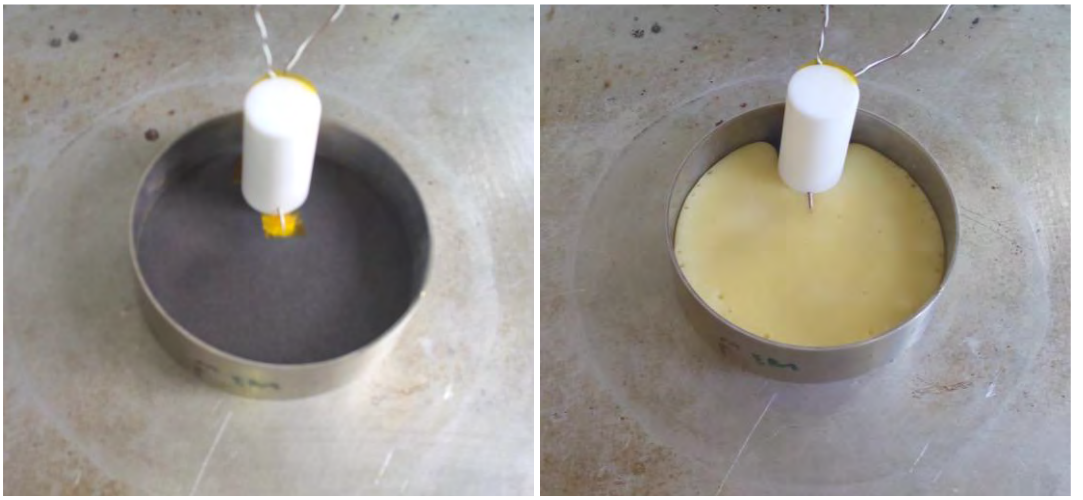

249

250 Fig. 3. Frying disk with type-K thermocouples and PTFE piece. The left picture shows the position of the bottom sensor fixed to the disk surface.
251 The right picture shows the other sensor measuring the temperature on the top surface of the pancake during the cooking process.

252 The frying disk with the cylindrical PTFE piece with the thermocouples inside (Fig. 3) is placed on the hot
253 surface. When the disk temperature is steady, the scales is set to zero and the dough is poured as fast as possible
254 using a syringe, trying to spread it uniformly. After a given time the pancake is removed from the disk and it is
255 placed inside a dark chamber, where a picture of the bottom face is taken with a conventional digital camera (no
256 flash, velocity ISO-80, focal 3.2mm, exposure time 1/640s). Different cooking times are tested, from 60 s to 240 s,
257 in order to measure the influence of the time in the browning development. The expansion of the pancakes cannot be
258 measured with enough accuracy, as from the same instant in which they are taken out from the frying pan they start
259 to shrink due to cooling and loss of stored vapor. Moreover the expansion is not completely uniform and different
260 thicknesses were observed. Therefore, the expansion is calculated theoretically; cf. eq. (16) in section 2.1.

3.2. Measurement of temperature, mass and water content

The measured temperatures inside the pancakes prepared on the uniform-heating rig at different surface temperatures from 180ºC to 260ºC, are shown in Fig. 4. The temperatures measured with the bottom thermocouple (solid lines) and the thermocouple at the top surface of the pancake at a height of 3.5 mm (dashed lines), are presented. The total cooking time in this case is 240 seconds. The bottom temperature curves exhibit an initial drop when the cold pancake dough is poured on the frying disk, where after they slowly rise towards the rig temperature, as expected. The temperature measured by the top thermocouple before pouring the dough presents a higher value with respect to the real ambient temperature, 25ºC, due to the heating of the PTFE piece which holds it. The pancake top surface approaches the water evaporation temperature, because this phase change consumes a high amount of energy and produces a cooling effect. As the pancake dries out, the evaporation effect is lower, and the temperature may exceed the evaporation temperature, as it is the case of a set temperature of 260ºC. No appreciable separation of the sensor from the top surface due to dough expansion was noticed during any experiment, and the repeatability of the measurements was also confirmed by comparison of the results obtained in different pancakes, cooked with same set temperatures of the uniform-heating rig, at different instants. This confirms that if there is some displacement, it has low influence, or it is the same in all experiments.

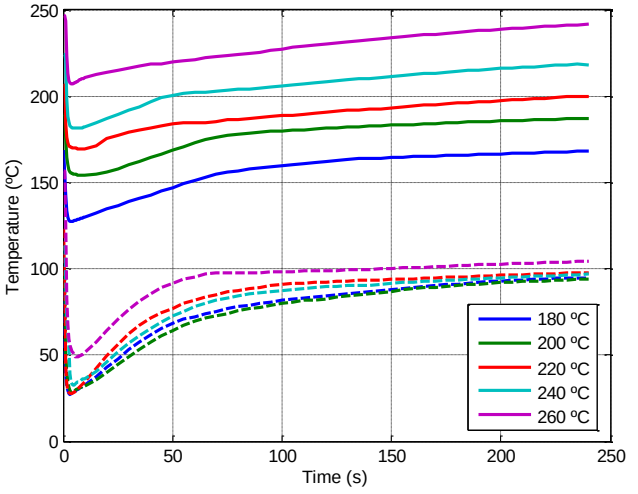

Fig. 4. Temperature evolution measured on the bottom surface of the pancake (continuous lines) and on the top surface of the pancake (dashed lines) using different temperatures of the uniform-heating rig.

As an example of the mass measurement, Fig. 5 shows the evolution of the normalized pancake mass during a

cooking process with different set temperatures from 180ºC to 260ºC, during 240s. The initial mass used for the normalization was measured with a conventional analytical balance as the difference between the mass of the syringe before and after pouring the dough. The jagged behavior of the presented lines is a consequence of oscillations of the weight measurement and the posterior median filter employed to eliminate spurious data.

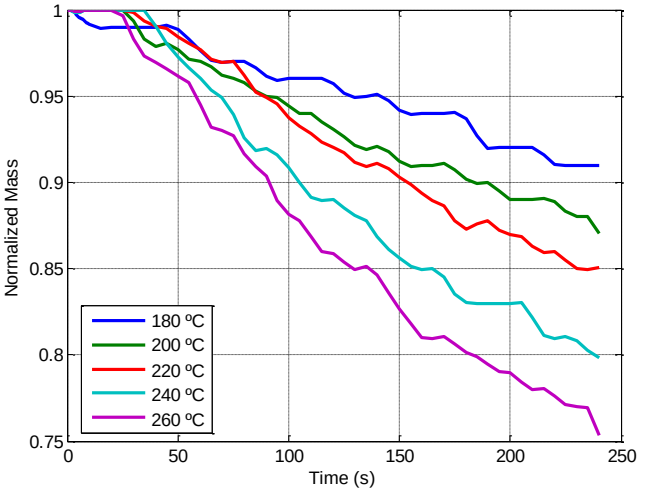

Fig. 5. Pancake total mass measured during the cooking process, using different temperatures of the uniform-heating rig.

3.3. Color extraction from computer vision system

The pictures of the pancakes are processed using Matlab in order to extract the browning information. A blue-colored background was employed in order to help the segmentation of the picture and obtain the colors of the pixels corresponding to the pancake. As it can be seen in Fig. 6, which corresponds to a pancake cooked using a set temperature of 240ºC during 180s, there is a wide variation of colors on the pancake surface, which is the result of the production of bubbles of water vapor in the interphase of the pancake product and the plate. These bubbles with different sizes generate insulation layers which slow down the increment of temperature in some zones of the product, producing a lower browning with respect to other zones which remained in contact with the plate. The regions of interest are the zones constantly in contact with the frying plate, and this must be taken into account in the color extraction process, since the color correlation is modeled from the evolution of the temperature measured on the disk surface.

Fig. 6. Picture of a pancake cooked using a set temperature of 240ºC during 180s in the uniform-heating rig. Images scale is 380 pixels per inch, the color space is sRGB.

Each picture is processed using the same algorithm in Matlab R2013a. First, a color space conversion from the original sRGB to the standard CIE L*a*b* is carried out. Then with the b* component a mask is obtained, which is used to suppress the image background. In order to extract the color which truly corresponds to the measured temperature, a region of interest is defined by segmentation, suppressing the lighter areas. The normalized histograms of the color components in the region of interest are shown in Fig. 7. The Gaussian curve which best fits each distribution is also plotted, as well as the mean value calculated with the distribution data (red vertical line). It can be seen that the mean of the Gaussian and the calculated mean are almost coincident, which confirms the good approximation of the normal distribution.

The mean values obtained for each color component L*, a* and b*, depending on the plate temperature and the time are shown in Fig. 8. The values have been converted to the commonly used range for the CIE L*a*b* color space, in which L* ranges from 0 to 100, and a*, b* range from -128 to 127. The blue lines correspond to experiments at the same cooking time in the temperature graphs (left-hand), and at the same temperature in the time graphs (right-hand). A different behavior of each component can be noticed. The only component which is strictly decreasing with time and temperature, according to the proposed model, is the component L*. In the case of a* and b* the tendency differs, and expression (22) is not adequate to explain the behavior of these color components. Thus, for simplification the values of a* and b* are calculated as the mean value of the experimental data.

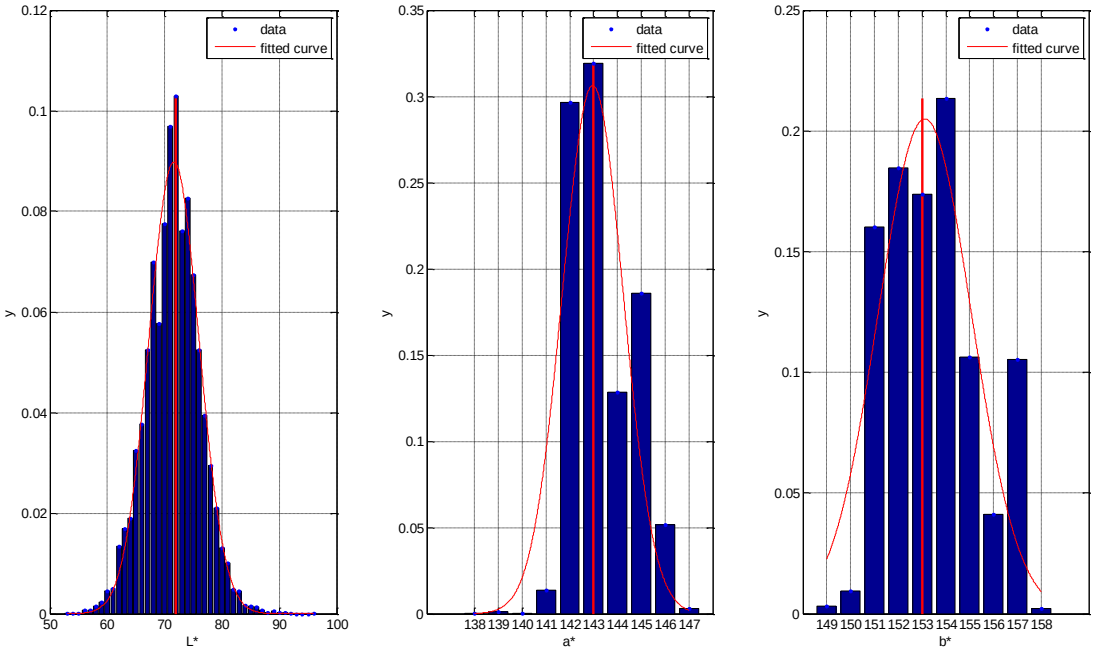

316

317 Fig. 7. Histograms of each color component obtained from the regions of interest. The Gaussian distribution which best fits each histogram is
318 shown.

319

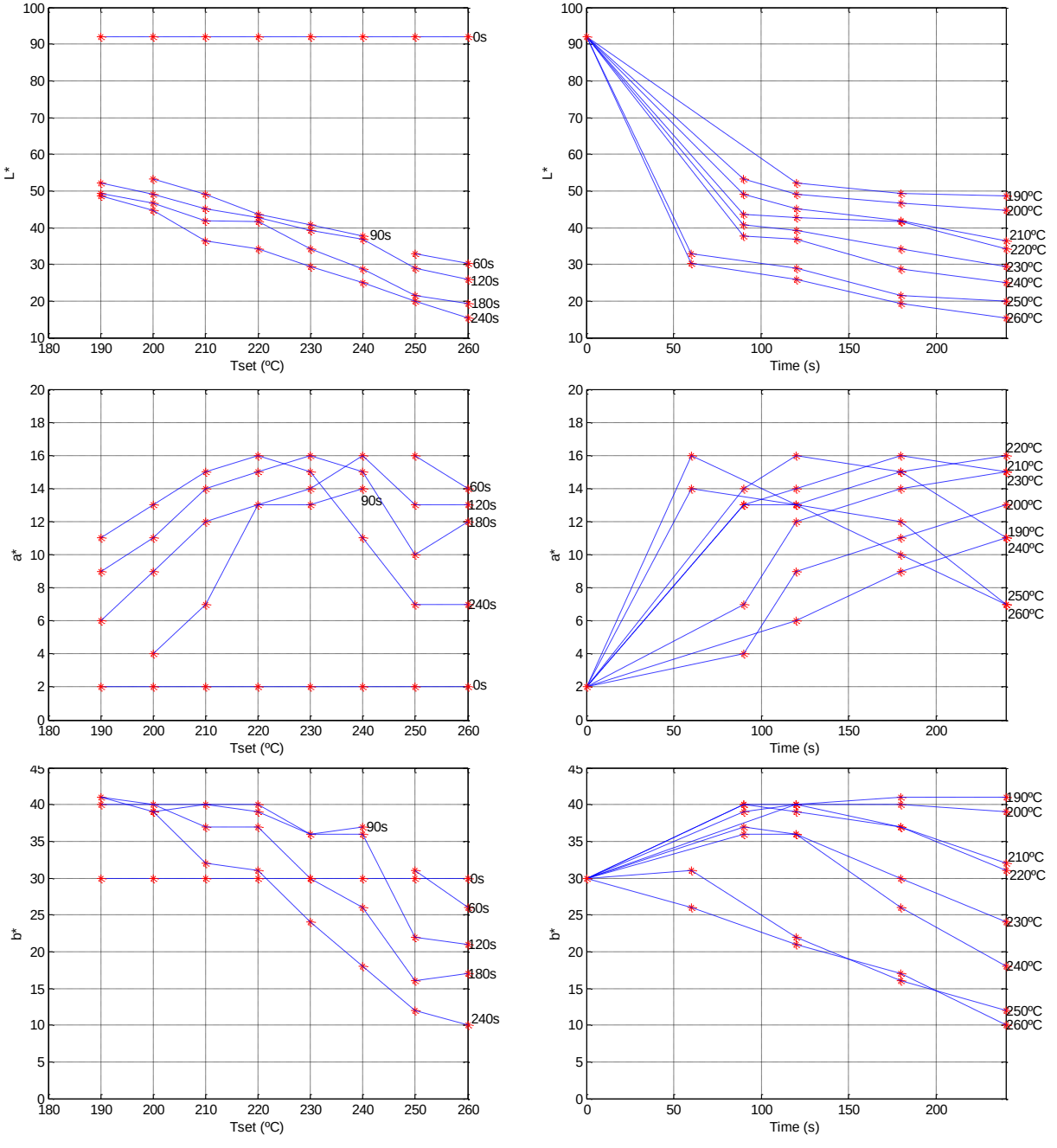

Fig. 8. Mean value of each measured color component L*a*b* depending on the set temperature and the cooking time. Blue lines represent data obtained from experiments with the same time on the left-hand plots, and with the same set temperature on the right-hand plots.

3.4. Parameter identification

The experimental data collection is used in the identification process of the heat and mass transfer model parameters and of the color correlation parameters. Because each model can be simulated independently, the

identification of each set of parameters is carried out separately.

3.4.1. Optimization for the finite element model COMSOL-Matlab

An optimization algorithm is implemented in Matlab in order to calculate the values of the model parameters which best fit the experimental measurements of temperature and mass loss. The algorithm uses the COMSOL-Matlab interface, and the optimization method used is the non-linear least squares method, using a trust-region-reflective algorithm. The objective function to minimize is the sum of the squared errors between the measured and calculated evolution of the temperature on top and bottom of the pancakes and of the normalized mass, taking into account different experiments with set temperature from 180 ºC to 260 ºC.

The built-in COMSOL modules "Heat transfer in solids" and "Transport of concentrated species" are used for modeling the cooking process. A time-dependent study solves the transient problem for the desired time. The model geometry is relatively simple, therefore a mapped mesh has been used in the whole model. A finer mesh is employed in the domain corresponding to the pancake, where the coupled thermal and mass transfer problem is solved, with elements of 1 mm in radial direction and 0.23 mm in axial direction. In the disk domain the elements are bigger in axial direction (1.25 mm), since heat conduction is higher and low temperature differences are expected. The total number of elements is 2207 domain elements plus 512 boundary elements. The time step is set to 1s, though for the first steps the software takes a lower time step of 1e-3s, which is increased as convergence is achieved. The selected solver is direct, fully coupled, with the default configuration given by the software.

The optimization variables and the obtained values are presented in Table 1. Examples of the fitting are shown in Fig. 9, in which the temperature evolution in the top and bottom surface of the pancake and the normalized mass are plotted for two set temperatures: 180ºC and 260ºC. The simulated curves are plotted as continuous lines, and the experimental data with asterisks. The good fitting of calculated and measured data demonstrates the accuracy of the results. The small differences in the normalized mass may be a consequence of having considered constant values of the diffusion coefficients for the vapor and liquid water, instead of including the effects of pressure or temperature, as presented by Datta (2007b). These coefficients determine the mass fraction of vapor which is contained inside the pancake (and the porosity), which affects the heat conductivity and the rate of water evaporation.

*3.4.2. Optimization of color model L*a*b**

For the calculation of the parameters of the browning development model, the measured temperature evolution

and the water content in the bottom surface of the pancake are employed. The water content is calculated using the finite element model for different set temperatures. The optimization algorithm uses equations (21) and (22) to minimize the error between the calculated and the measured color component L* for each cooking time and set temperature.

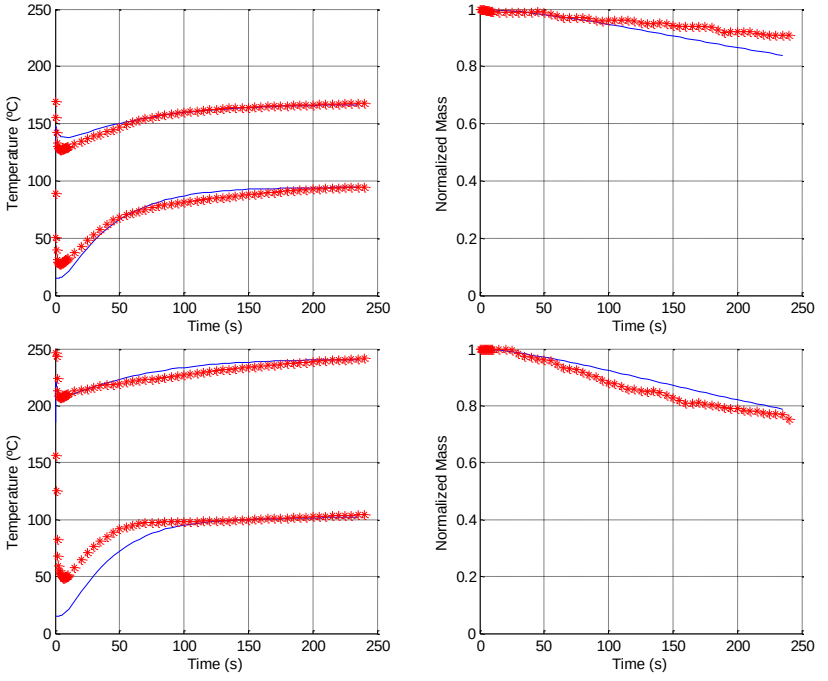

Fig. 9. Comparison of measured and calculated temperature and mass evolution using the parameter values from the identification algorithm, for different set temperatures: 180ºC and 260ºC.

Table 1. Parameter values obtained from the optimization algorithm.

Parameter	Value	Units
σ_{ev}	5.44e-4	s^{-1}
k_θ	1.61e3	-
g_ε	1.2	-
k_v	3.8e-3	$m \cdot s^{-1}$
h_c	460	$W \cdot m^{-2} \cdot K^{-1}$
D_l	1e-9	$m^2 \cdot s^{-1}$
D_v	1.05e-5	$m^2 \cdot s^{-1}$

The fitted curves can be seen in Fig. 10, which shows the dependence of the color value with the cooking time

and the set temperature as a parameter. The error between the fitted curves and the measured values is a result of the high dispersion of the measured data and the approximation of the proposed model based on reaction kinetics. The parameter values for the fitting of the L* component, and the mean values of a* and b* are shown in Table 2. With these values, the correlations can be used to simulate the color distribution when cooking the pancake in an induction hob with known power distribution.

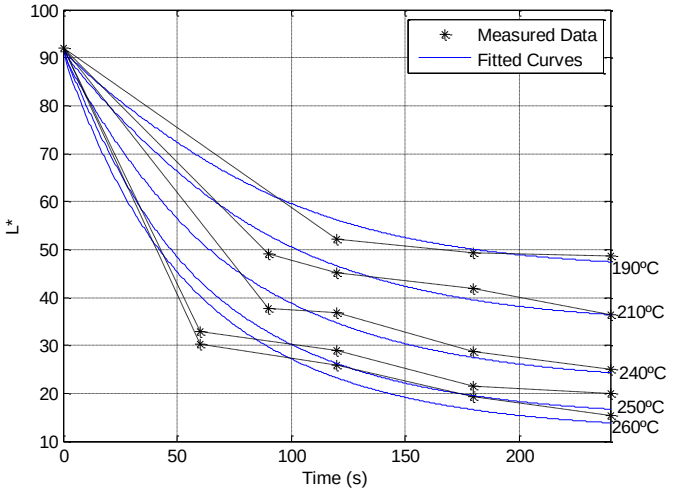

Fig. 10. Fitting of the color component L* obtained using the parameters obtained from the identification.

Table 2. Parameter values for the correlations of color component L* and mean values of color components a* and b*.

Parameter	Value	Units
L_0	92	-
k_1	15.4	s^{-1}
k_2	2.22e-14	s^{-1}
A_1	2.22e-14	K
A_2	2.16e3	K
a^*	12.6	-
b^*	32.7	-

4. Application of the model to pancake cooking in non-uniform heating domestic cookers

Considering that the pancake behavior is independent of the source which heats the cooking vessel, the proposed two-dimensional model of pancake cooking can be used for different types of heating technologies in domestic stoves. To achieve this, the heat source needs to be well characterized, so that it can be used as an input in the model.

As an example, two different commercial stoves are considered: an induction hob (BOSCH PIE645B18E) and a radiant stove (Balay 3EE721LS). The induction hob consists of a coil of diameter 18 cm, heating a conventional frying pan of 19 cm, made of ferromagnetic steel with known thermal and electromagnetic properties. The power distribution generated in the pan can be calculated (Carretero et al., 2015; Sanz-Serrano et al., 2016) and used directly in the finite element model proposed in this work. As it can be seen in Fig. 11 (left), the power distribution is not completely uniform: the heat generation is null in the center and outside the coil, which may cause unevenness in the temperature distribution. The radiant stove has a cooker composed of two independent resistors in concentric configuration. The internal has a diameter of 12 cm and the external a maximum diameter of 21 cm. The power distribution, transferred by conduction from the ceramic glass to the frying pan, is shown in Fig. 11 (right) (Sanz-Serrano et al., 2016). In this case the frying pan has a diameter of 21 cm, the same as the external resistor in the cooking zone.

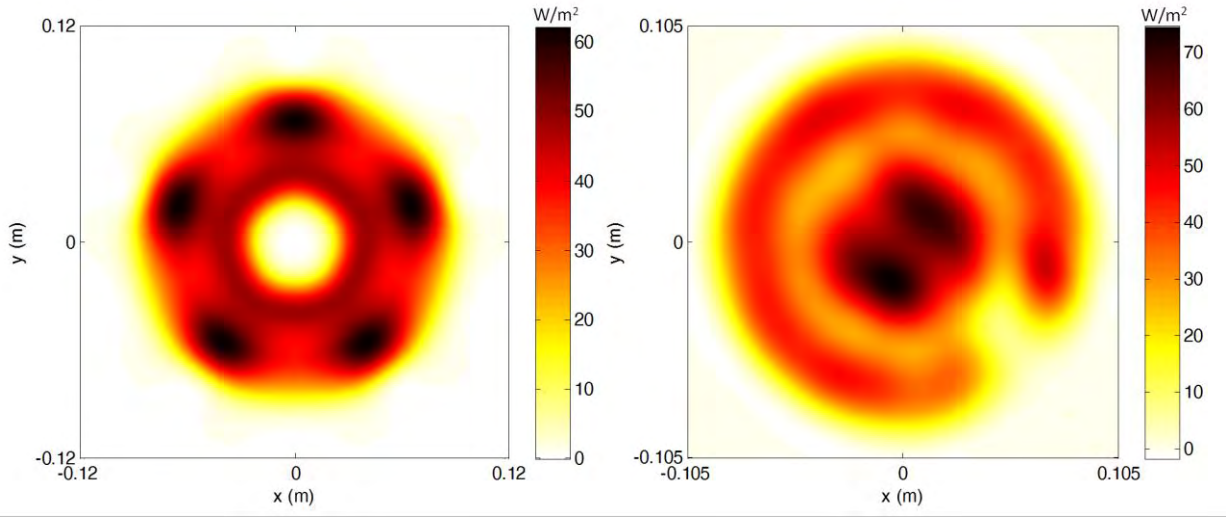

Fig. 11. Power distribution generated in a C-45 ferromagnetic steel disk of diameter 24 cm with a conventional induction cooker with a coil of 18 cm of diameter (left); power distribution transferred from the ceramic glass to a frying pan in a double cooker of 12/21 cm of an electric stove (right).

A cooking situation supplying a total power of 1000 W to a pan of 19 cm of diameter with the mentioned inductor is simulated, and the pancake color is predicted. Since the power distribution is not completely axisymmetric and slightly fluctuates in the angular direction, the average power distribution in this direction is computed and the radial profile is used in the model. The radial profiles of normalized power distribution, temperature of the bottom of the frying pan, and L* component of the color distribution obtained from the simulation after 60s are shown in Fig. 12 (left). Since the pan diameter is bigger than the coil diameter, the heating of the outer area is insufficient, obtaining high temperature gradients in the base of the pan and an inadequate cooking result, shown by the differences in the predicted color of the pancake. It can also be noticed that despite the center of the pan is not directly heated by the coil, the heat conduction from the hotter area towards the center helps to make uniform in the temperature.

A cooking process with a frying pan of 21 cm of the same material used for the induction hob is simulated with the radiant stove as the heating element. The average in angular direction of the power distribution shown in Fig. 11 (right) is also computed and used as input in the model. The power needed for cooking is lower than in the case of the induction cooker, provided that the ceramic glass has been previously heated up to the normal operation temperature (around 450ºC); therefore the power considered is 600 W, supplied continuously during time. The radial profiles of power distribution and temperature in the bottom of the frying pan, and the L* color component obtained are shown in Fig. 12 (right). In this case, the power distribution is higher in the central part of the cooker, due to the unequal power transferred by each one of the resistances. This generates a higher temperature difference in the center of the pan with respect to the border, compared with the induction cooker. The resulting color distribution follows the same behavior as the temperature. The maximum difference obtained in the L* value is 43, which is similar to the maximum difference obtained for the induction hob, 37. However, the deviation for the electric stove is higher, which makes the color distribution less uniform, producing a perception of lower quality in the cooking result, as can be seen in Fig. 13.

In order to assess these simulation results obtained with the proposed model, a set of 16 pancakes are cooked using each one of the aforementioned stoves. For the induction hob, the power supplied by the inductor is 1000 W and the cooking time for the first face of the pancake is 60 s (afterwards the pancakes are flipped and further cooked during 15 s). For the radiant cooker, the average power supplied by the resistors is 600 W and the cooking time for

421 the first face of the pancake is 70 s (as the pan is slightly bigger in this case). It can be considered that the color
422 distribution on the first face remains constant after cooking the second face. A picture of one of the pancakes, and
423 the values of the different color components L*a*b* along four radii taken every 90º are shown in Fig. 14 for the
424 induction hob, and in Fig. 15 for the radiant cooker. The simulated color components have been also plotted in black
425 continuous line for comparison, showing good agreement in the L* component.

426 The measured colors present a noisy behavior due to the irregular surface of the pancakes and the small vapor
427 bubbles which alter the contact between the product and the frying pan during the cooking process. A lighter color
428 area near the center of the pancake, effect of a bigger vapor bubble, can also be seen in the case of the induction hob,
429 which is similar to the effects observed in the experiments with the uniform-heating rig, shown in Fig. 6. The
430 appearance of these bubbles seems to have a random occurrence, therefore their location cannot be predicted with
431 the proposed model. However, since they provide no information about the uniformity of the temperature
432 distribution, they should be disregarded for the evaluation of the cookers. Using the model for the calculation of the
433 color distribution in different situations, the color differences are computed instead of measured, avoiding also the
434 effect of differences in the evaluator's perception.

435 It is evident from the simulation that the color distribution is closely related to the temperature distribution in the
436 pan during the cooking process. Therefore, it might be possible to test the heaters' design by measuring the
437 temperature of the surface of an empty pan for example using an IR camera. However in order to correctly evaluate
438 the heating uniformity it is necessary to account for the effect of the food on the pan temperature and, despite the
439 robustness of the camera measurement, it is impossible to measure the temperature distribution in the pan while the
440 food is being prepared. Moreover, the temperature distribution measured at a given time is not as representative as
441 the measurement or calculation of the final color distribution, which depends on the whole temperature history
442 during the cooking process.

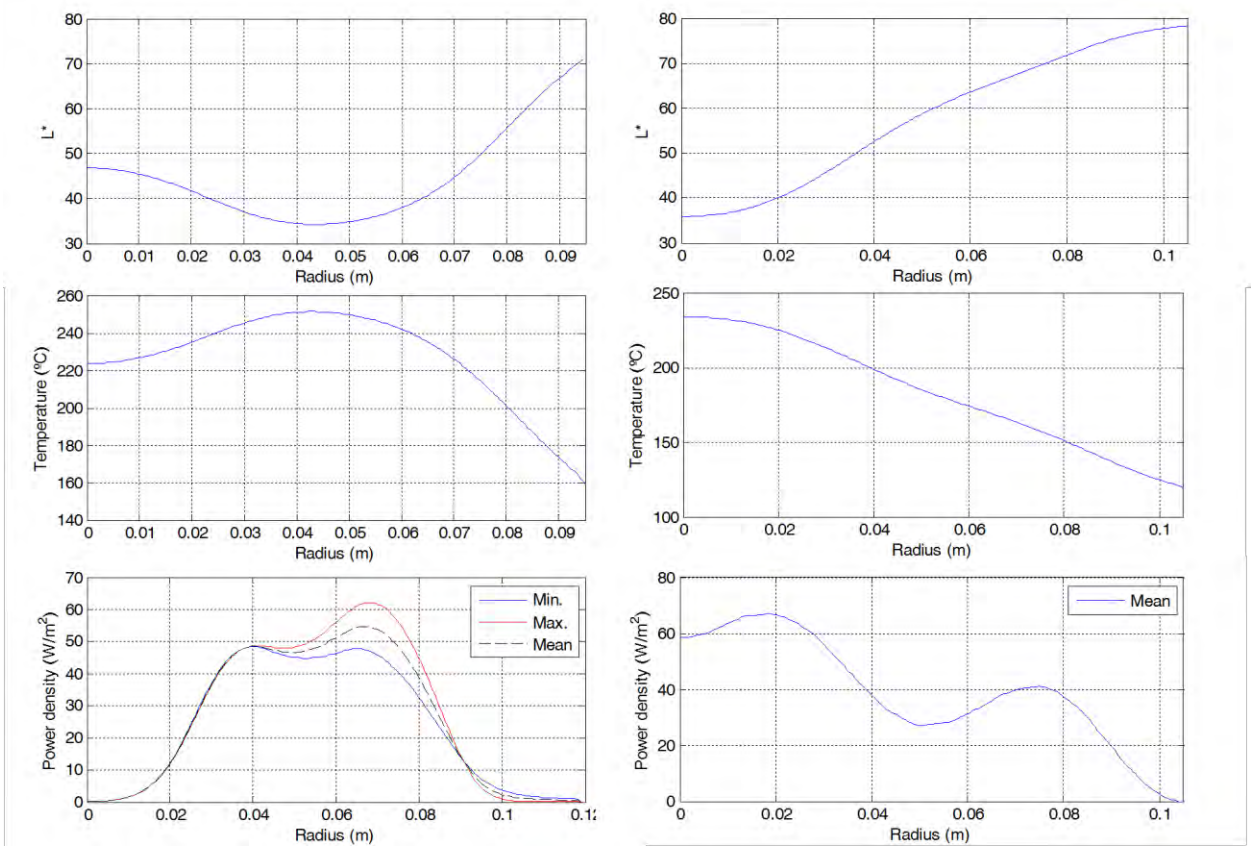

Fig. 12. Radial profiles of power density distribution, temperature in the bottom of the frying pan and L* component obtained from simulation of a cooking process with: an inductor of 18 cm heating a 19 cm pan during 60s supplying 1000 W (left); a double radiant cooker of 12/21 cm heating a 21 cm pan (right) during 70s supplying 600W.

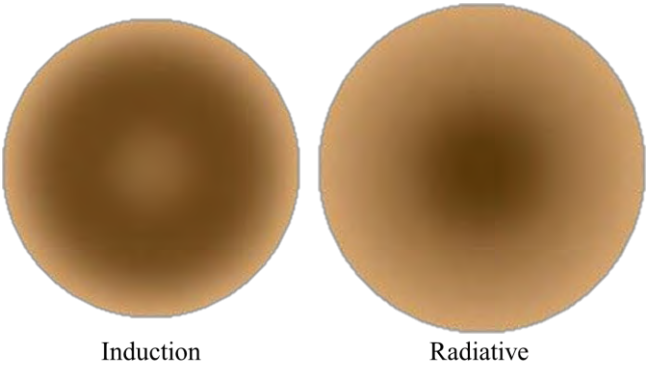

Fig. 13. Simulated pancakes for an induction cooker and an electric stove, using the same type of frying pan and cooking time. The color is obtained from the conversion of calculated L*a*b* to RGB for visualization.

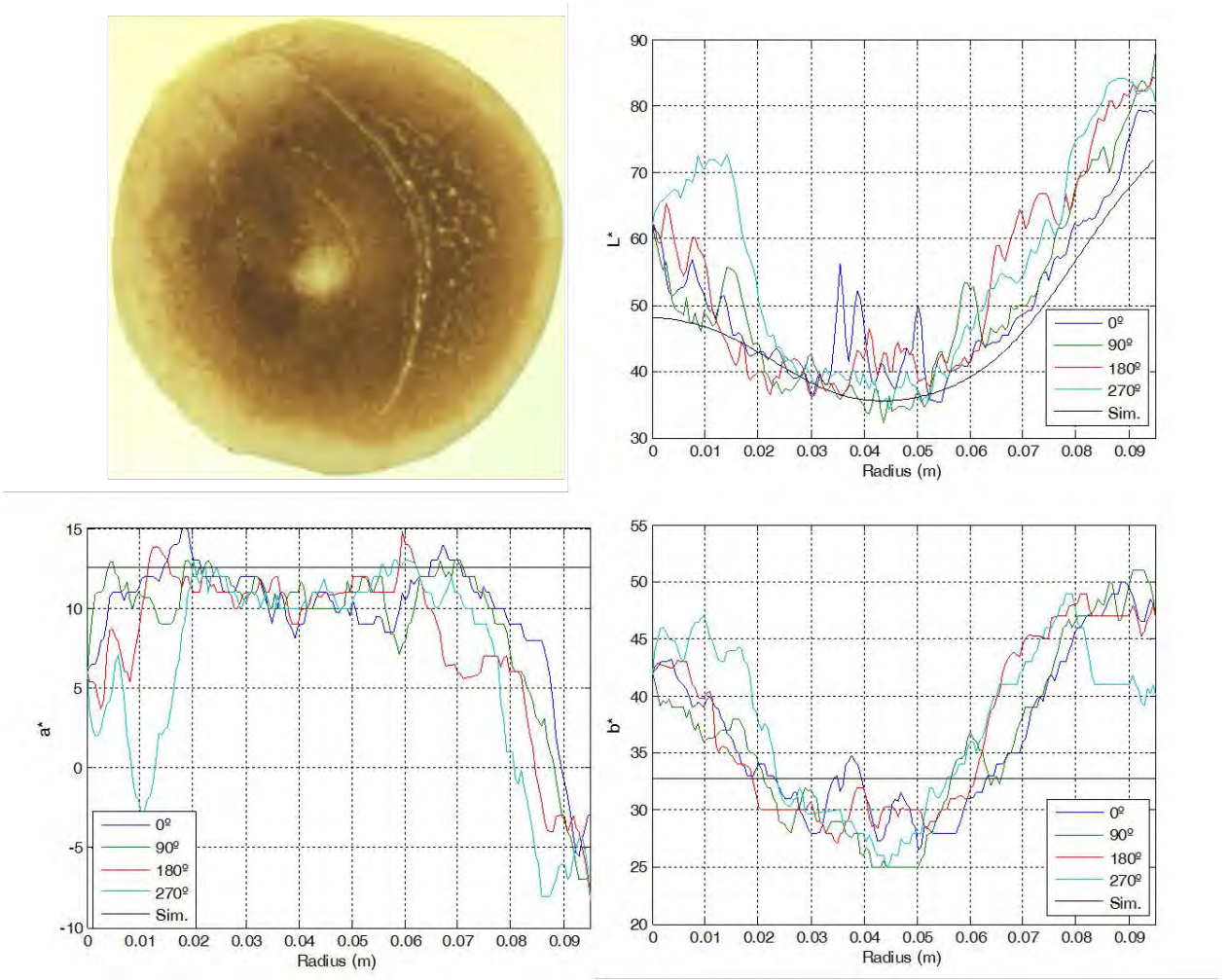

Fig. 14. Pancake cooked in a pan of 19 cm of diameter made of ferromagnetic steel heated with an inductor cooker of 18 cm. Radial profiles of color components L*a*b* measured and simulated.

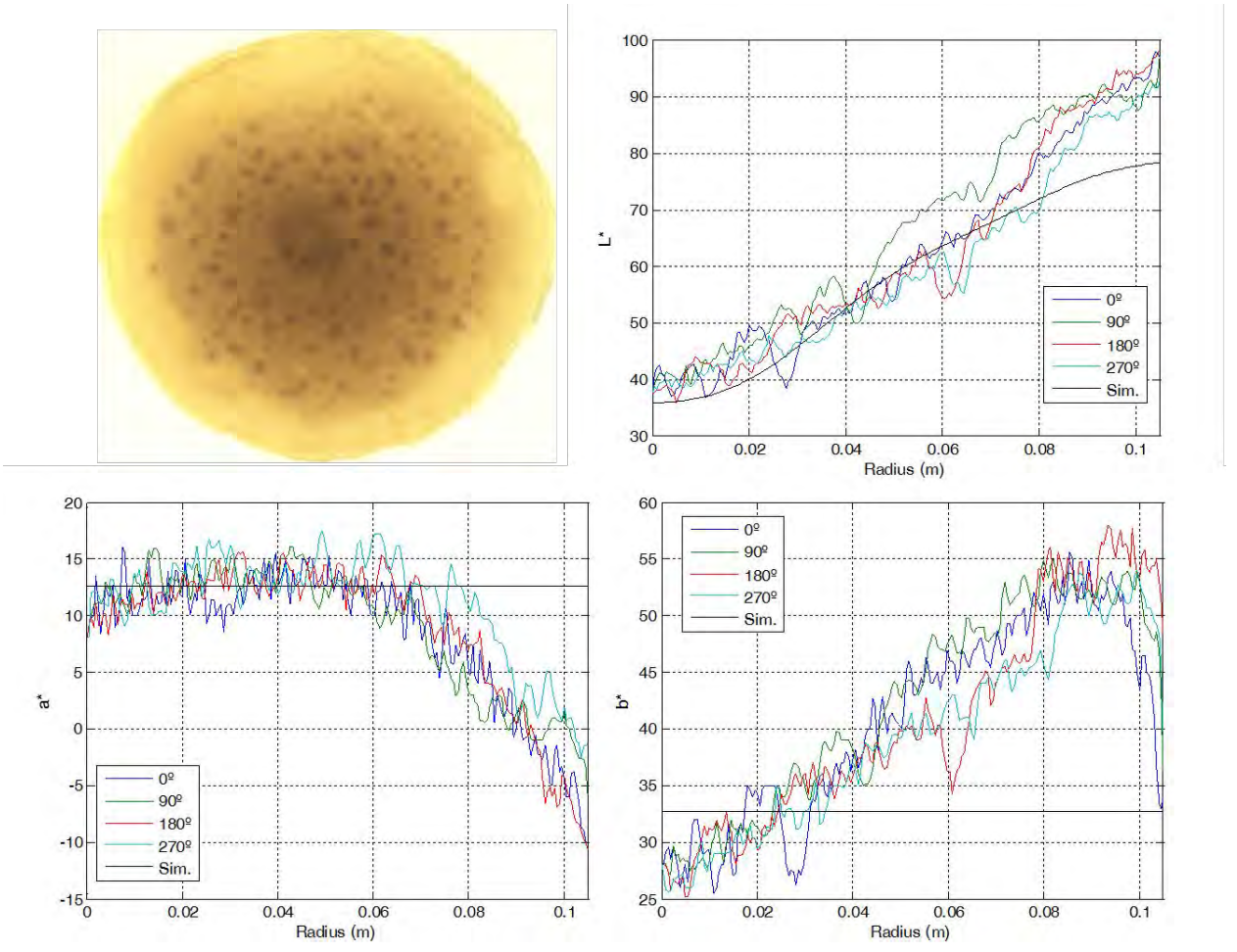

Fig. 15. Pancake cooked in a pan of 21 cm of diameter made of ferromagnetic steel heated with a double radiant cooker of 12/21 cm. Radial profiles of color components L*a*b* measured and simulated.

5. Conclusions

A two-dimensional model of heat and mass transfer and browning development in pancake cooking has been proposed. The main contribution of this work is the consideration of a non-uniform heating in the modeling, inspired by the real situation existing in current domestic cookers. Thus, the influence of the type of heating source and the frying pan are also included in the model. Moreover combining a transport model and a browning development model gives a more complete tool for the study of the contact pan-frying process.

The proposed model can be used for predicting the cooking result when using a given domestic cooker with a non-uniform heating in the food. Thus, the performance of such a stove can be evaluated without developing a real prototype and testing it experimentally, saving costs and accelerating the design process. In this work a particular

induction cooker and a radiant cooker of an electric stove have been considered, however alternative configurations and technologies could be further studied.

The color correlations of the browning development show a good agreement in the L* component. The evolution of the a* and b* components with the cooking process is relatively small but also non-linear, and its behavior cannot be represented by the selected model based on first order kinetics. However the average value calculated from the experimental data can be used to reproduce the changes in the browning when predicting the pancake color. The insulating effect of vapor bubbles in the interphase between the frying pan and the dough on the color was observed in the experiments. The light-color zones produced by these bubbles cannot be predicted with the proposed model, however since their appearance seem to be independent of the heating uniformity of the cooker, it is reasonable to ignore them for the evaluation of the cooker performance. The maximum color difference obtained for the induction cooker and the radiant cooker is similar, despite the color distribution with the first one is more uniform. In general, if the power is distributed towards the outer area of the pan, the cooking result is better than if it is concentrated in the center.

As future work, the model could be also used to evaluate different features of interest of the cooking process which are difficult to measure, such as the local temperature evolution and water content distribution, the energy employed in the water evaporation, the influence of the materials employed in the cooking vessel over the cooking efficiency or the effect of modifying the dough recipe.

Acknowledgements

Authors want to thank Food Production Engineering Group, National Food Institute of Denmark, for offering their facilities and valuable technical assistance during a three months' stay for author Sanz-Serrano.

This work has been partially supported by project RTC-2014-1847-6 (RETOS-COLABORACION), from Ministerio de Economia y Competitividad, Spain, and by grant AP2013/02769 from Ministerio de Educacion, Cultura y Deporte, Spain.

References

AEN/CT N 213 Electrodomesticos, 2014. Household electric cooking appliances - Part 2: Hobs - Methods for measuring performance. http://www.aenor.es/aenor/normas/normas/fichanorma.asp?tipo=N&codigo=N0054329

Ashokkumar, S., Adler-Nissen, J., 2011. Evaluating non-stick properties of different surface materials for contact frying. J. Food Eng. 105, 537–544. doi:10.1016/j.jfoodeng.2011.03.018

Bergman, T.L., Lavine, A.S., Incropera, F.P., Dewitt, D.P., 2011. Fundamentals of heat and mass transfer, seventh ed. ed, Dekker Mechanical Engineering. John Wiley & Sons.

Broyart, B., Trystram, G., Duquenoy, A., 1998. Predicting colour kinetics during cracker baking. J. Food Eng. 35, 351–368. doi:10.1016/S0260-8774(98)00021-1

Bushuk, W., Mehrotra, V.K., 1977. Studies of Water Binding by Differential Thermal Analysis. II. Dough Studies using the Melting Mode. Cereal Chem. 54, 320–325.

Carretero, C., Acero, J., Alonso, R., Burdio, J., 2015. Normal Mode Decomposition of Surface Power Distribution in Multiple Coil Induction Heating Systems. IEEE Trans. Magn. 52, 1–1. doi:10.1109/TMAG.2015.2487883

Datta, A.K., 2007a. Porous media approaches to studying simultaneous heat and mass transfer in food processes. II: Property data and representative results. J. Food Eng. 80, 96–110. doi:10.1016/j.jfoodeng.2006.05.012

Datta, A.K., 2007b. Porous media approaches to studying simultaneous heat and mass transfer in food processes. I: Problem formulations. J. Food Eng. 80, 80–95. doi:10.1016/j.jfoodeng.2006.05.013

Feyissa, A.H., Christensen, M.G., Pedersen, S.J., Hickman, M., Adler-Nissen, J., 2015. Studying fluid-to-particle heat transfer coefficients in vessel cooking processes using potatoes as measuring devices. J. Food Eng. 163, 71–78. doi:10.1016/j.jfoodeng.2015.04.022

Feyissa, A.H., Gernaey, K. V., Ashokkumar, S., Adler-Nissen, J., 2011. Modelling of coupled heat and mass transfer during a contact baking process. J. Food Eng. 106, 228–235. doi:10.1016/j.jfoodeng.2011.05.014

Fluoroproducts, D., 1996. Teflon PTFE Fluoropolymer Resin: Properties Handbook. DuPont Fluoroproducts.

Gökmen, V., Açar, Ö.Ç., Arribas-Lorenzo, G., Morales, F.J., 2008. Investigating the correlation between acrylamide content and browning ratio of model cookies. J. Food Eng. 87, 380–385. doi:10.1016/j.jfoodeng.2007.12.029

Gupta, T.R., 2001. Individual heat transfer modes during contact baking of Indian unleavened flat bread (chapati) in a continuous oven. J. Food Eng. 47, 313–319. doi:10.1016/S0260-8774(00)00135-7

León, K., Mery, D., Pedreschi, F., León, J., 2006. Color measurement in L∗a∗b∗ units from RGB digital images. Food Res. Int. 39, 1084–1091. doi:10.1016/j.foodres.2006.03.006

Martins, S.I.F.S., Jongen, W.M.F., Van Boekel, M. a J.S., 2000. A review of Maillard reaction in food and implications to kinetic modelling. Trends Food Sci. Technol. 11, 364–373. doi:10.1016/S0924-2244(01)00022-X

Nesvadba, P., 2014. Thermal properties of unfrozen foods, in: Engineering Properties of Foods. Taylor & Francis Group, pp. 223–245.

Pham, H.N., Fujita, H., Ozaki, K., Uchida, N., 2012. Estimating Method of Heat Distribution Using 3-D Resistance Matrix for Zone-Control Induction Heating Systems. IEEE Trans. Power Electron. 27, 3374–3382. doi:10.1109/TPEL.2011.2179984

Purlis, E., 2010. Browning development in bakery products - A review. J. Food Eng. 99, 239–249. doi:10.1016/j.jfoodeng.2010.03.008

Purlis, E., Salvadori, V.O., 2009. Modelling the browning of bread during baking. Food Res. Int. 42, 865–870. doi:10.1016/j.foodres.2009.03.007

Sanz-Serrano, F., Sagues, C., Llorente, S., 2016. Inverse modeling of pan heating in domestic cookers. Appl. Therm. Eng. 92, 137–148. doi:10.1016/j.applthermaleng.2015.09.084

Saxholt, E., Christensen, A.T., Møller, A., Hartkopp, H.B., Hess Ygil, K., Hels, O.H., 2008. Danish Food Composition Databank, revision 7 [WWW Document]. Dep. Nutr. Natl. Food Institute, Tech. Univ. Denmark. URL http://www.foodcomp.dk/

Ulbrich, M., Flöter, E., 2014. Impact of high pressure homogenization modification of a cellulose based fiber product on water binding properties. Food Hydrocoll. 41, 281–289. doi:10.1016/j.foodhyd.2014.04.020

Zheng, C., Sun, D.-W., Zheng, L., 2006. Recent developments and applications of image features for food quality evaluation and inspection – a review. Trends Food Sci. Technol. 17, 642–655. doi:10.1016/j.tifs.2006.06.005

Zorrilla, S.E., Singh, R.P., 2003. Heat transfer in double-sided cooking of meat patties considering two-dimensional geometry and radial shrinkage. J. Food Eng. 57, 57–65. doi:10.1016/S0260-8774(02)00273-X